

Contents		Page no
General information	Instrumental information	3
Figure S1	^{13}C CP/MAS	4
Figure S2	BJH pore size distribution of the networks	5

Role of redox-active centres and charge density in covalent organic networks for energy storage applications as a high-performance asymmetric supercapacitor

Koustab Chowdhury^a, Nikita Ahlawat^b, Love Bansal^b, Sayantan Sarkar^a, Plabani Samanta^a, Rajesh Kumar^{*b}, Suman Mukhopadhyay^{*a}

^aDepartment of Chemistry, IIT Indore, Indore, Madhya Pradesh-453552, India.

^bDepartment of Physics, IIT Indore, Indore, Madhya Pradesh-453552, India.

Figure S3	Deconvoluted XSP spectra of N 1s and C 1s	5
Figure S4	TGA data of the networks	6
Figure S5	EDX profile of the networks	7
Figure S6	Element mapping of the networks	8
Figure S7	FTIR spectra of the networks after acid-base treatment	9
Figure S8	Scan rate-dependent CV curves of the CON-2 electrode	9
Figure S9	Scan rate-dependent CV curves of the CON-3 electrode	10
Figure S10	Variation of GCD plots at various current densities for the CON-2 electrode	10
Figure S11	Variation of GCD plots at various current densities for the CON-3 electrode	11
Figure S12	Variation of specific capacitance as a function of current density for the CON-2 electrode.	11
Figure S13	Variation of specific capacitance as a function of current density for the CON-3 electrode.	12
Table 1	Comparison with other conjugated state-of-the-art electrode materials	13
Movie clip S1-S5	S1-S5	14

Instruments:

FTIR analysis was carried out using PerkinElmer's Spectrum II spectrometer. Nuclear magnetic resonance (NMR) spectra were recorded using an advanced III 500 MHz Ascend Bruker Biospin machine at ambient temperature with CDCl_3 as the solvent. ^{13}C -CP/MAS was carried out using an ECZR series 600 MHz NMR by JEOL. TGA experiments were carried out using a Mettler Toledo thermal analyzer with a heating rate of $10\text{ }^\circ\text{C}/\text{min}$ under N_2 atm. Morphological investigations were carried out using JEOL JSM-7400F field emission scanning electron microscopy. EDX and element-mapping analyses were performed at an accelerating voltage of 15 kV. Gas adsorption-desorption isotherms were carried out using a Quantachrome Autosorb iQ2 Brunauer-Emmett-Teller (BET) surface area analyzer. PXRD of the networks was performed on Empyrean, Malvern Panalytical, by $\text{Cu K}\alpha$ radiation with a 2θ range of 5° to 80° and a step size of 0.02° . X-ray Photoelectron Spectroscopy was performed by a Physical Electronics-made PHI 5000 VersaProbe III ($\text{Mg K}\alpha$ X-rays, $h\nu = 1253.6\text{ eV}$). All the electrochemical measurements were carried out using Metrohm-Multi AutolabTM M204 potentiostat.

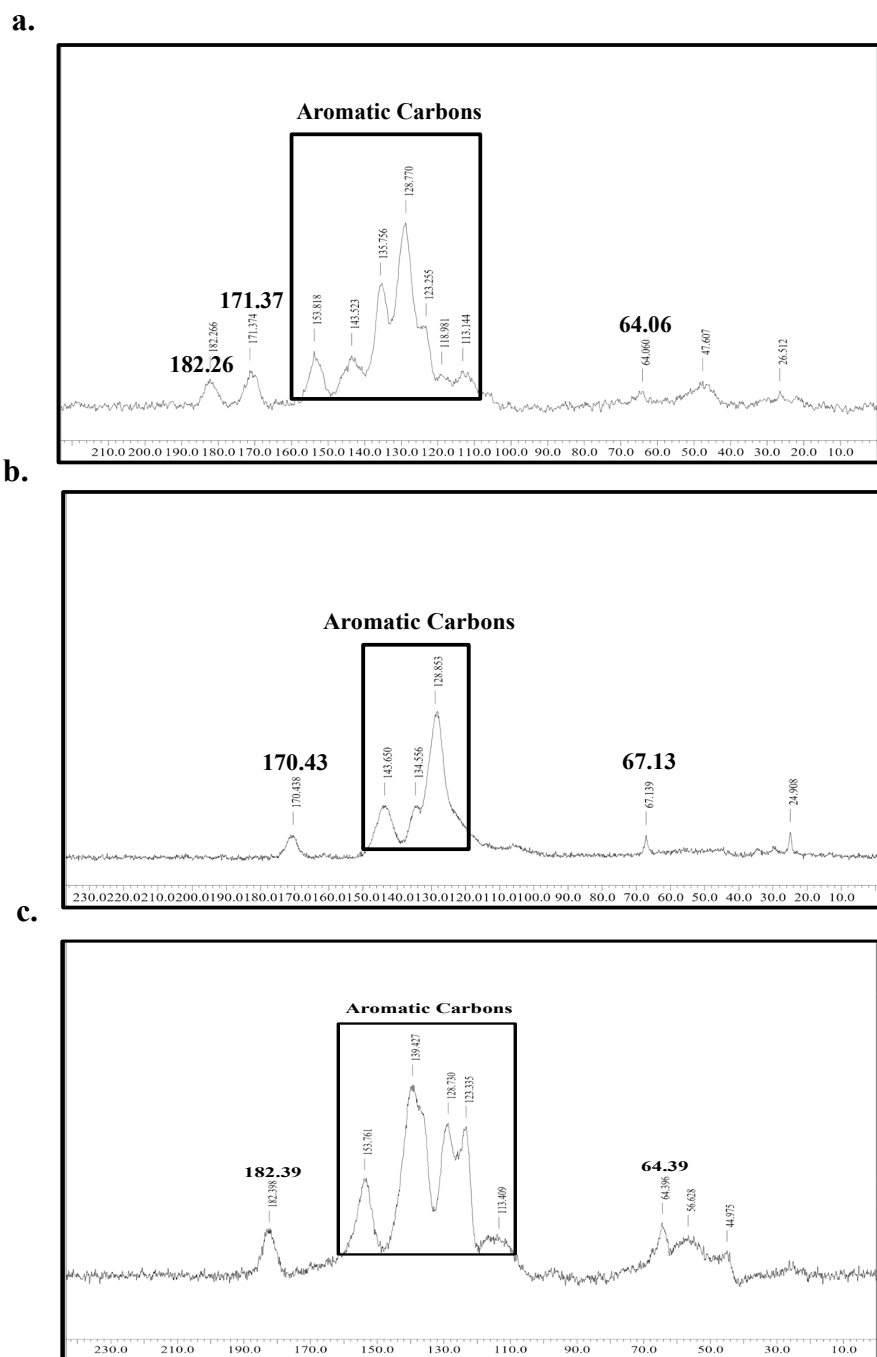


Figure S1. ^{13}C - CP/MAS spectra of (a) CON-1, (b) CON-2, and (c) CON-3.

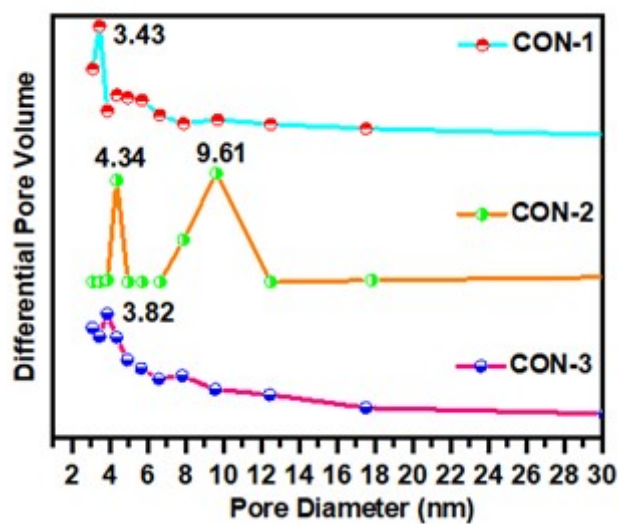


Figure S2. BJH pore size distribution profiles of the polymeric networks.

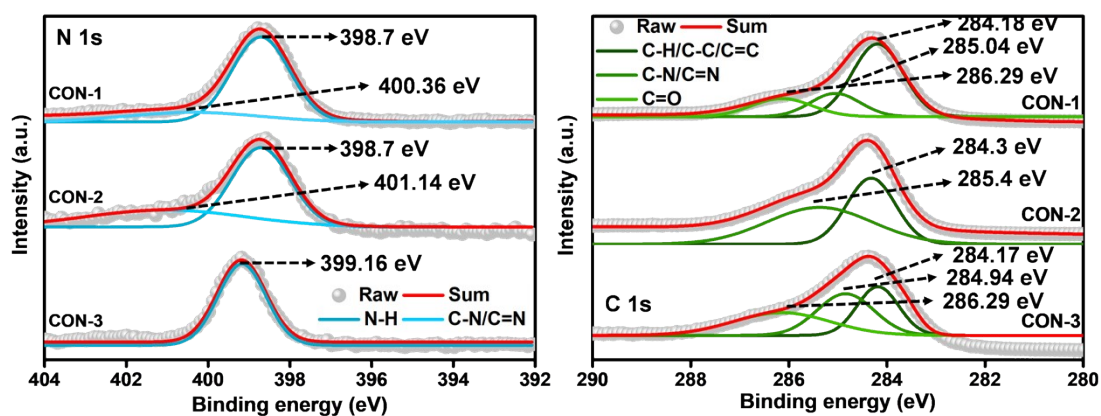


Figure S3. Deconvoluted spectra of (a) N 1s, (b) C 1s.

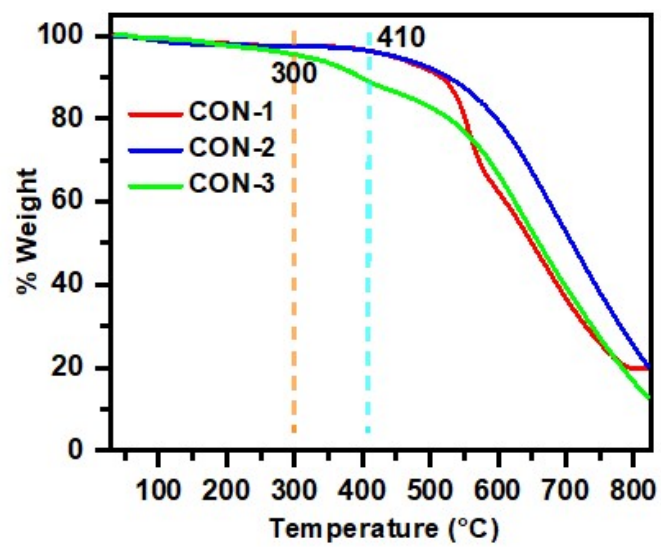


Figure S4. TGA data of the networks.

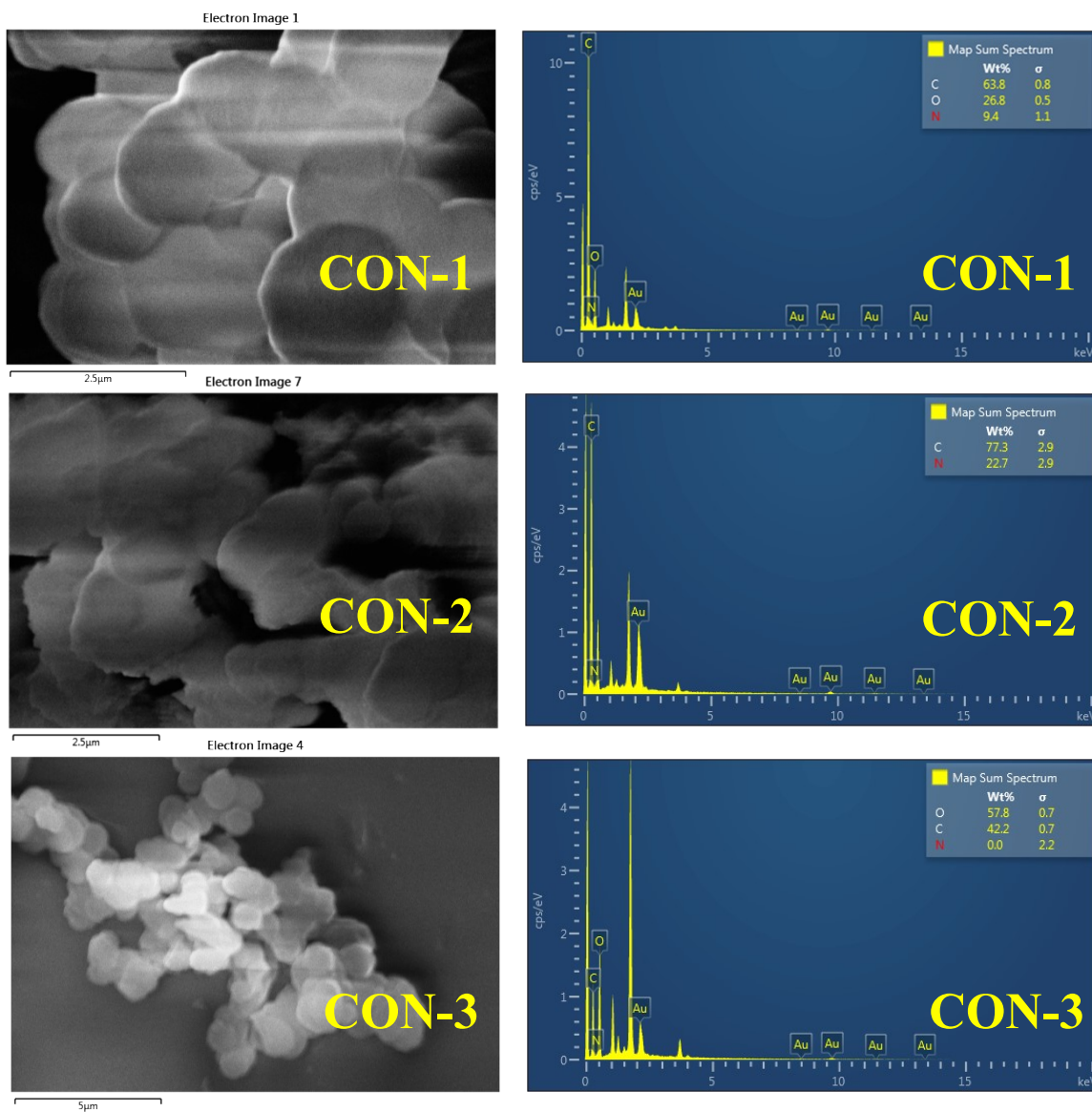


Figure S5. EDX profile of the networks, CON-1, CON-2, and CON-3.

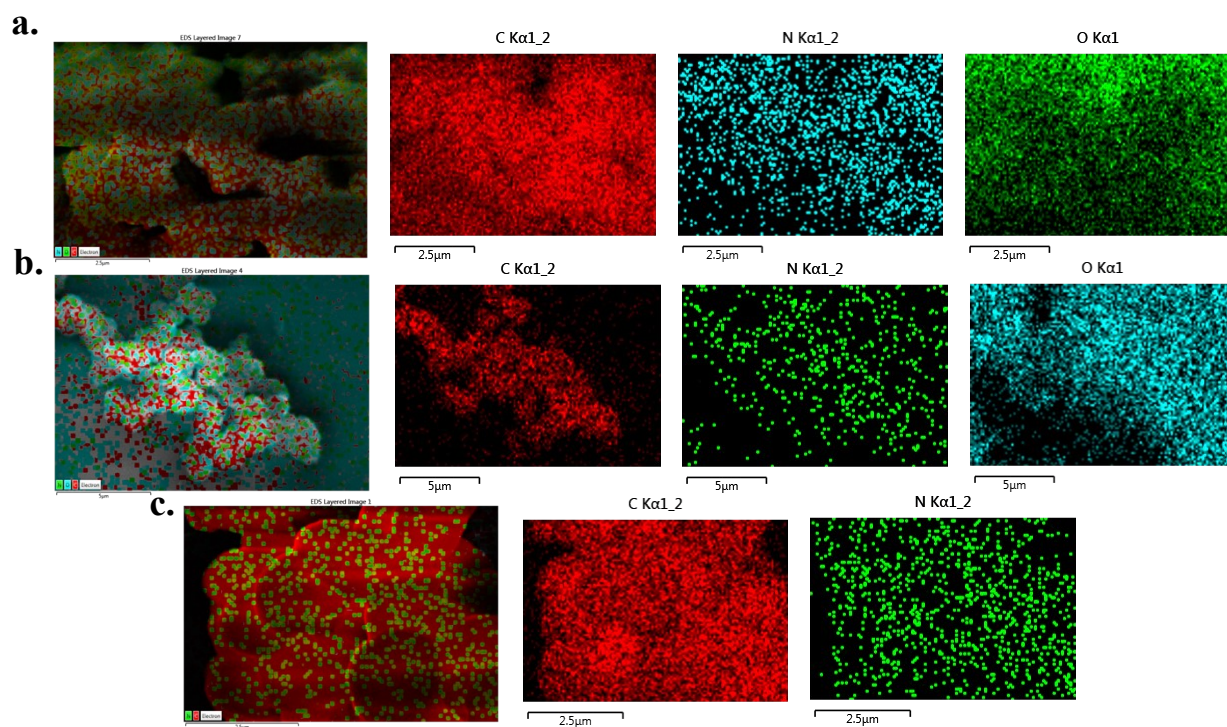


Figure S6. Element mapping of (a) CON-1, (b) CON-3, (c) CON-2.

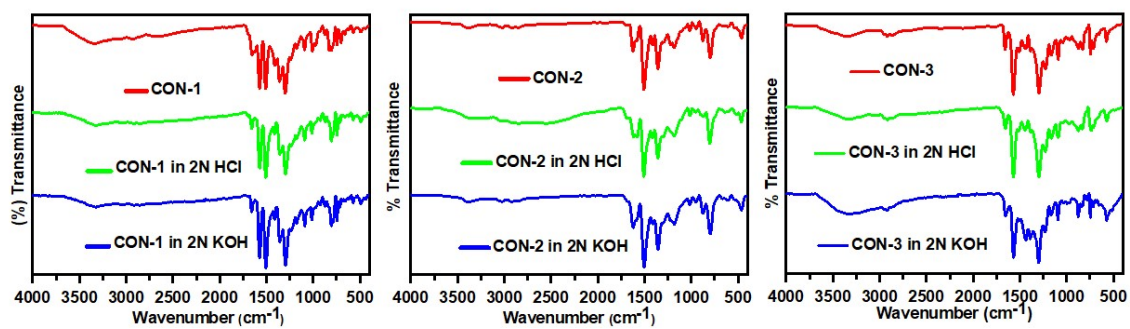


Figure S7. FTIR spectra of the networks after treatment with acid and base.

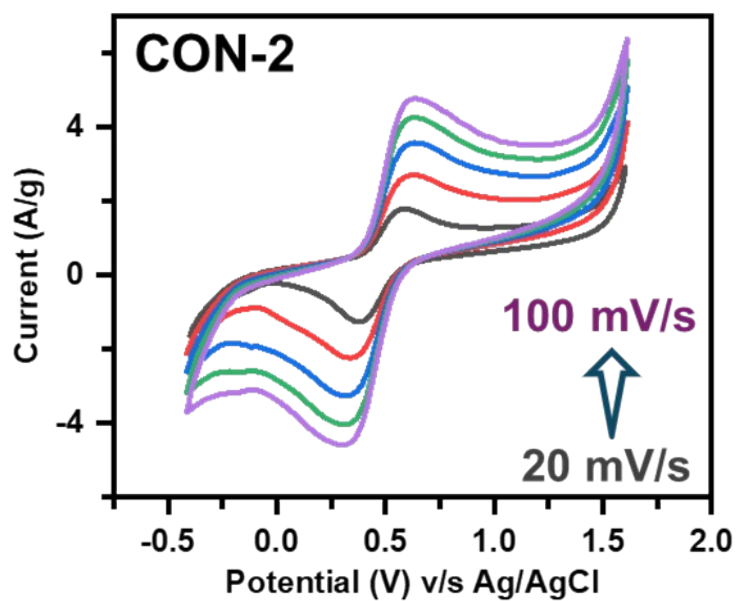


Figure S8. Scan rate-dependent CV curves of the CON-2 electrode.

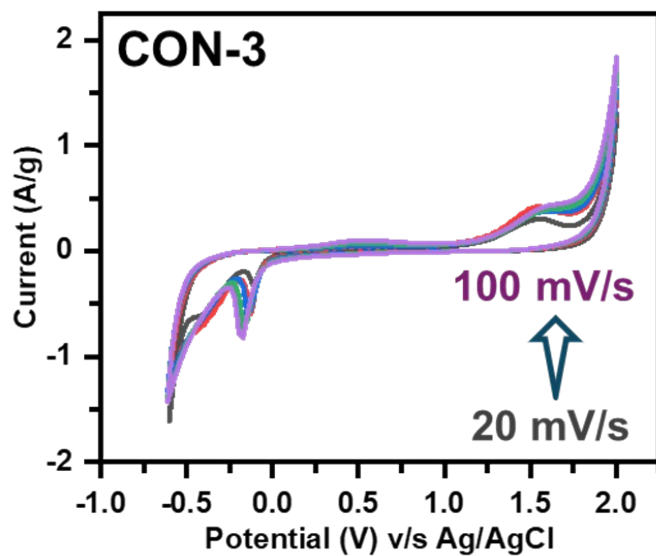


Figure S9. Scan rate-dependent CV curves of the CON-3 electrode.

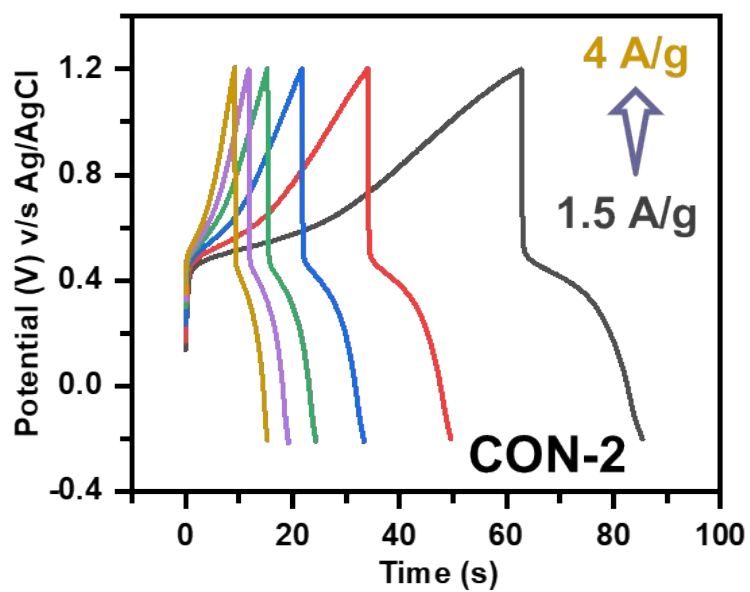


Figure S10. Variation of GCD plots at various current densities for the CON-2 electrode.

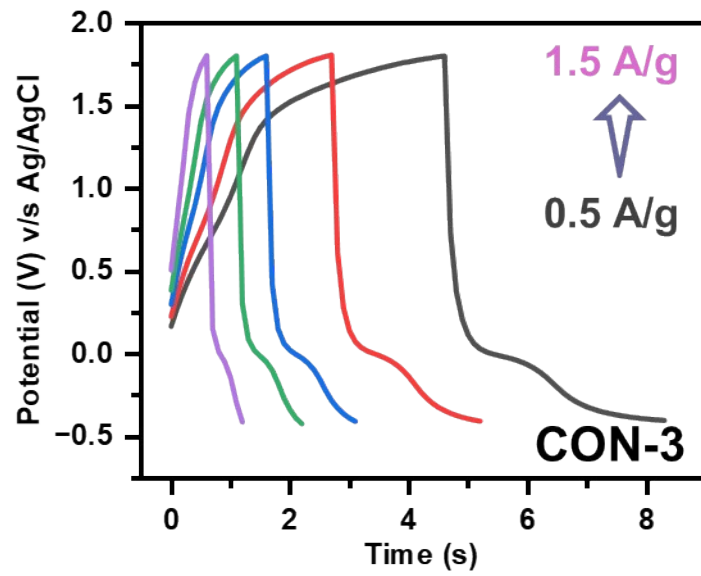


Figure S11. Variation of GCD plots at various current densities for the CON-3 electrode.

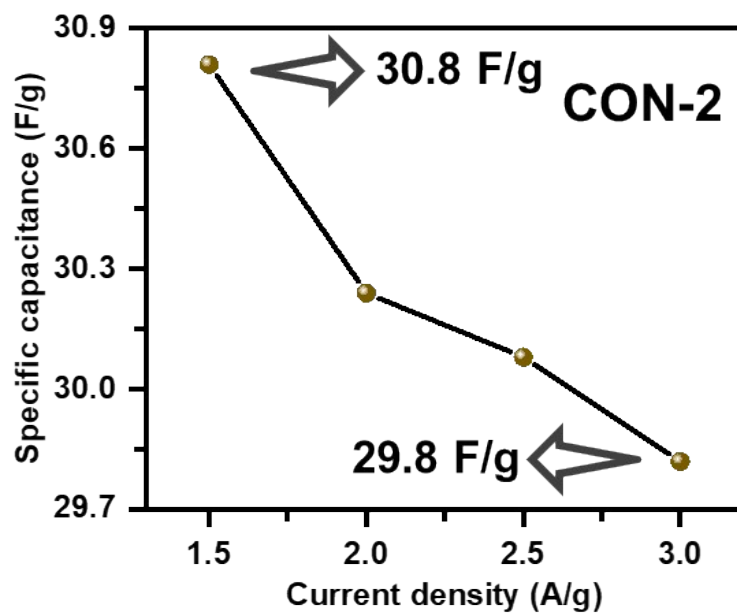


Figure S12. Variation of specific capacitance as a function of current density for the CON-2 electrode.

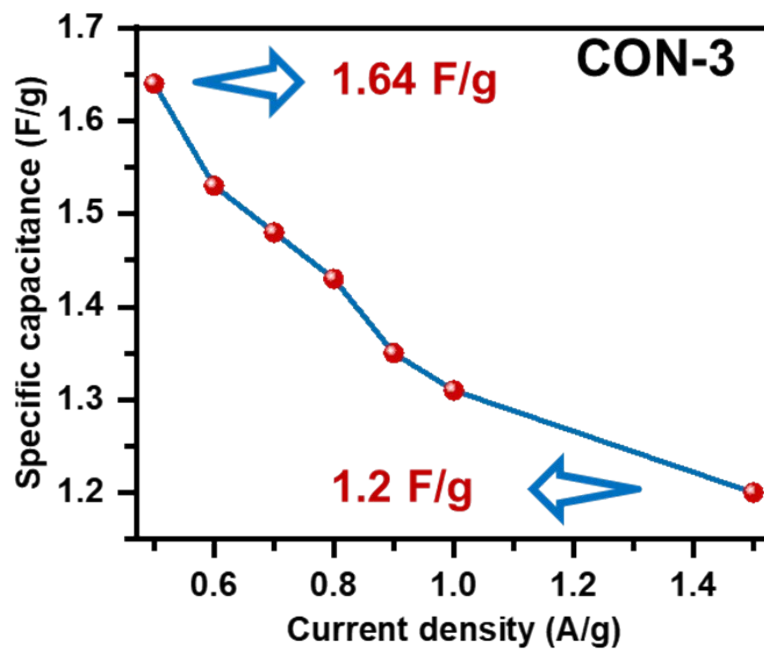


Figure S13. Variation of specific capacitance as a function of current density for the CON-3 electrode.

Table 1. Comparison with other conjugated state-of-the-art electrode materials.

	Electrode materials	Specific Capacitance and current density (Three electrode)	Specific capacitance and current density in a solid-state device	Electrolyte	Reference
1	TpOMe-DAQ (Conjugated)	135 F/g and 0.35 A/g	84 mF/cm ² and 0.25 mA/cm ² (Symmetric)	2 M H ₂ SO ₄	1
2	IISERP-COF-10 (Conjugated)	547 F/g and 0.5 A/g	92 mF/cm ² and 0.5 mA/cm ²	1 M H ₂ SO ₄	2
3	DQ ₁ Da ₁ Tp COF (Conjugated)	111 F/g and 1.56 mA/cm ²	8.5 mF/cm ² and 0.39 mA/cm ²	1 M H ₂ SO ₄	3
4	TDFP-1 (Conjugated)	354 F/g and 2 mV s ⁻¹	-	0.1M H ₂ SO ₄	4
5	PANI/TCOF-2 (Conjugated)	275 F/g and 0.5 A/g	-	1 M H ₂ SO ₄	5
6	TaPa-py-COF (Conjugated)	209 F/g and 0.5 A/g	102 F/g and 0.5 A/g	1 M H ₂ SO ₄	6
7	CC-DAQ-CMP (Conjugated)	184.25 F/g and 1 A/g	94 F/g and 1 A/g Asymmetric	6 M KOH	7
8	1KT-TP-TOF (Conjugated)	61 F/g and 0.2 A/g		1 M H ₂ SO ₄	8
9	BD-TP-COF (Conjugated)	20 F/g and 0.2 A/g		1 M H ₂ SO ₄	8
10	BD-TF-COF (conjugated)	25 F/g and 0.2 A/g		1 M H ₂ SO ₄	8
11	TPA-TPA-COF-1(Conjugated)	51.3 F/g and 0.2 A/g		H ₂ SO ₄	9
12	DAAQ- TFP COF(Conjugated)	48±10 F/g and 0.1 A/g		1M H ₂ SO ₄	10
13	CON-1 (Non-Conjugated)	70 F/g and 0.5 A/g	72.9 mF/cm ² and 0.1 mA/cm ² (asymmetric)	0.5 M H ₂ SO ₄	This work
	CON-2 (Non-Conjugated)	30.08 F/g and 1.5 A/g	-	0.5 M H ₂ SO ₄	This work
	CON-3 (Non-Conjugated)	1.64 F/g and 0.5 A/g	-	0.5 M H ₂ SO ₄	This work

Movie clip S1: Videography showing the lighting up of a red LED using the ASC device.

Movie clip S2: Videography showing the lighting up of a yellow LED using the ASC device.

Movie clip S3: Videography showing lighting up green LED using the ASC device.

Movie clip S4: Videography showing lighting up a blue LED using the ASC device.

Movie clip S5: Videography showing lighting up white LED using the ASC device.

Reference:

- 1 A. Halder, M. Ghosh, A. Khayum M, S. Bera, M. Addicoat, H. S. Sasmal, S. Karak, S. Kurungot and R. Banerjee, *J. Am. Chem. Soc.*, 2018, 140, 10941–10945.
- 2 S. Haldar, R. Kushwaha, R. Maity and R. Vaidhyanathan, *ACS Mater. Lett.*, 2019, 1, 490–497.
- 3 A. Khayum M, V. Vijayakumar, S. Karak, S. Kandambeth, M. Bhadra, K. Suresh, N. Acharambath, S. Kurungot and R. Banerjee, *ACS Appl. Mater. Interfaces*, 2018, 10, 28139–28146.
- 4 P. Bhanja, K. Bhunia, S. K. Das, D. Pradhan, R. Kimura, Y. Hijikata, S. Irle and A. Bhaumik, *ChemSusChem*, 2017, 10, 921–929.
- 5 T. K. Dutta and A. Patra, *Chem. – Asian J.*, 2021, 16, 158–164.
- 6 A. M. Khattak, Z. A. Ghazi, B. Liang, N. A. Khan, A. Iqbal, L. Li and Z. Tang, *J. Mater. Chem. A*, 2016, 4, 16312–16317.
- 7 B. Luo, Y. Chen, Y. Zhang and J. Huo, *New J. Chem.*, 2021, 45, 17278–17286.
- 8 M. Li, J. Liu, Y. Li, G. Xing, X. Yu, C. Peng and L. Chen, *CCS Chem.*, 2020, 3, 696–706.
- 9 A. F. M. EL-Mahdy, C.-H. Kuo, A. Alshehri, C. Young, Y. Yamauchi, J. Kim and S.-W. Kuo, *J. Mater. Chem. A*, 2018, 6, 19532–19541.
- 10 C. R. DeBlase, K. E. Silberstein, T.-T. Truong, H. D. Abruña and W. R. Dichtel, *J. Am. Chem. Soc.*, 2013, 135, 16821–16824.